DIFFUSION COUPLE STUDIES OF THE Ni–Bi–Sn SYSTEM

G. Vassilev[a,*], N. Milcheva[a,b], M.C. Record[c], R. Mancheva[b]

[a] University of Plovdiv, Faculty of Chemistry, Plovdiv, Bulgaria
[b] Medical University of Plovdiv, Faculty of Pharmacy, Plovdiv, Bulgaria
[c] University of Äix-Marseille, Institute of Materials Microelectronic and Nanosciences of Provence, Faculty of Sciences and Technology, IM2NP, Marseille, France

Abstract

Investigations of Ni–Bi–Sn system were performed in order to inquire the phase diagram and to assess some diffusion kinetic parameters. For this purpose diffusion couples consisting of solid nickel (preliminary electroplated with tin) and liquid Bi–Sn phase were annealed at 370 °C. Three compositions (0.8, 0.6 and 0.4 mole fractions Sn) of the Bi–Sn melts were chosen. Annealing times from 24 to 216 h were applied. The phase and chemical compositions of the contact zone were determined by means of scanning electron microscope.

It was confirmed that the diffusion layers consist mainly of Ni_3Sn_4 but other intermetallic phases grow as well. For the first time metastable Ni–Sn phases as NiSn and $NiSn_8$ ($NiSn_9$) were observed in metallurgical alloys (i.e. not in electroplated samples). The existence of a ternary compound previously reported in the literature was confirmed. More than one ternary Ni–Bi–Sn compounds might possibly be admitted.

A growth coefficient of $(2.29 ± 0.02) \times 10^{-15}$ m^2 s^{-1} was obtained. It was found that the apparent activation energy for diffusion layers growth $(18 ± 8$ kJ $mol^{-1})$ is inferior to that one assessed at growth from solid state Bi–Sn mixtures $(88 ± 12$ kJ $mol^{-1})$.

Keywords: Metals and alloys; Diffusion couples; Phase diagrams

1. Introduction

Tin and bismuth are prospective for use as lead-free solders' components while nickel or other transition metals frequently appear as substrate. In this connection, one should mention a few contributions to kinetic, wetting or microstructure issues of samples obtained by putting in contact Bi–Sn alloys and Ni substrates [1-10].

The above cited literatures demonstrate the industrial interest in these alloys. Nevertheless, the fundamental (phase diagram and thermodynamic) properties of a materials' system must be known in order to better modify the desired qualities. In this relation, the end-binary systems continue to be subject of intensive studies. For example, Ipser et al. [11, 12] have recently studied the phase equilibria in the Ni–Sn system and have found some previously unknown modifications of the compound Ni_3Sn_2. Moreover, one should be aware that metastable phases ($NiSn_9$) [13] and NiSn were obtained by electrochemical deposition of nickel-tin alloys. The -same phase was reported by Rooksby [14] also in electroplated samples and could be considered as metastable extension of the equilibrium compound Ni_3Sn_2 over its homogeneity range [15,16]. Nevertheless, these metastable phases have not been observed in alloys obtained by metallurgical way.

Bi–Sn and Bi–Ni phase diagrams have also been subject to relatively recent experimental research [17–20]. Investigations of phase equilibria, thermochemical and other properties of Bi–Sn–X (X= Ni, Ti) systems were performed by Vassilev et al. [21–27]. Indications of the formation of a ternary intermetallic compound (IMC) with approximate formula Ni_7Sn_2Bi [23, 25] and of the appearance of a ternary eutectic [24, 25, 27] have been found. Another (allegedly quaternary) IMC with composition $Au_2Ni_{15}Sn_{77}Bi_6$ was reported by Cho et al. [9].

The aim of the present study is to inquire the construction of the phase diagram, the appearance of ternary compounds, the stability of phases such as $NiSn_9$ and NiSn in metallurgical alloys, the mutual solubility of the third component (tin or bismuth) in the respective nickel-bismuth and nickel–tin binary phases.

---

* Corresponding author: gpvassilev@excite.com

Dedicated to the memory of Professor Zbigniew Moser

2. Review of previous (Ni)/(Bi,Sn) and (Ni)/(Sn) interfacial reactions studies

Normally, three Ni–Sn (Ni_3Sn, Ni_3Sn_2 and Ni_3Sn_4) and two Ni–Bi (NiBi and $NiBi_3$) intermetallic compounds (IMC) compete among them to form and grow into (Ni)-phase from Bi–Sn melts with various compositions. The situation is even more intricate as the concentration region of Ni_3Sn_2 is complex [11, 12] and metastable phases [13-16] might appear together with the stable IMC (Table 1).

The kinetics of the interfacial reactions occurring between Ni-substrate and (Bi, Sn) candidate solders, having approximately eutectic composition (61.9 at. % Sn) were investigated at 85, 100, 120, and 135 °C by Chen et al. [2], at 180, 240, 300, 360, and 420 °C by Tao et al. [3], at 145 and 185 °C by Young and Duh [4], at 70, 90, 100, 120 °C, by Yoon et al. [5], at 125 °C by Cho et al. [9] and by Lin et al. [10] at 250, 260, and 280 °C. Lee et al. [7] and Wang et al. [8] used other than eutectic compositions of the Bi–Sn solders: 4–13 at. % Sn (at 300 °C), and 37, 64 and 91 at. % Sn (at 150 °C), respectively. It has been found, generally, that single Ni_3Sn_4–layer is produced by the reaction of

(Ni) and solid or liquid Bi–Sn solder with eutectic composition [1–5, 8–10] while $NiBi_3$-layer was formed [7] from melts with Bi-content greater than 96.5 at. % Bi.

Bader et al. [33] have observed the formation of Ni_3Sn_4, Ni_3Sn_2 and Ni_3Sn phases when Sn solidifies between two thin Ni-layers. Thus, this is the so-called "reaction of isothermal solidification" and is not precisely diffusion couple study. Some deviations from the parabolic growth were observed and explained with the influence of grain-boundary diffusion and the influence of the small grain size [33]. Shen et al. [34] also discussed the growth mechanism of Ni_3Sn_4-layers. No induction times for the growing phase nucleation were reported.

Concerning the reaction kinetics, parabolic rule (i.e. diffusion controlled growth) was observed [2, 3, 5, 8, 10] except at 420 °C [3]. In the latter case linear kinetics (i.e. chemical reaction controlled growth) was reported.

At a constant temperature (T, K), the contact zone growth could be represented by the expression (1) if a very fast nucleation rate of the reactionary growing phase(s) would be assumed:

Table 1. *Description of the binary phases relevant to the Bi–Ni–Sn system [13, 14, 18, 20, 28-32].*

Phase	Binary system	Homogeneity range / at. %	Pearson Symbol	Space group	Prototype	Reference
(Ni)	Ni–Sn	≈0–11 at. % Sn	$cF4$	$Fm\bar{3}m$	Cu	[18, 20]
	Ni–Bi	≈0 at. % Bi				[28]
*(Ni)	Ni–Sn	10–18 at. %Sn				[29]
(αSn)	Ni–Sn	≈ 100 at. % Sn	$cF8$	$Fd\bar{3}m$	C (diam.)	[28, 30]
	Bi–Sn	≈ 100 at. % Sn				
(βSn)	Ni–Sn	≈ 100 at. % Sn	$tI4$	$I4_1/amd$	βSn	[28, 30]
	Bi–Sn	≈ 87–100 at. % Sn				
Ni_3Sn_HT	Ni–Sn	23–27 at. % Sn	$hP16$	$Fm\bar{3}m$	BiF_3	[28]
Ni_3Sn_LT	Ni–Sn	24–26 at. % Sn	$hP8$	$P6_3/mmc$	Mg_3Cd	[28]
Ni_3Sn_2_HT	Ni–Sn	38–41 at. % Sn	$hP6$	$P6_3/mmc$	Ni_2In	[28]
Ni_3Sn_2_LT	Ni–Sn	39–43 at. % Sn	$hP4$	$P6_3/mmc$	NiAs	[28]
*NiSn	Ni–Sn	48–51 at.% Sn			NiAs	[14, 31]
Ni_3Sn_4	Ni–Sn	56–57 at. % Sn	$mC14$	$C2/m$	CoGe	[28]
*Ni_3Sn_4	Ni–Sn	60–75 at. % Sn				[29]
*$NiSn_8$	Ni–Sn	75–90 at. % Sn		$C2/m$	Ni_3Sn_4	[29]
*$NiSn_9$		66–97 at. % Sn				[13, 32]
(Bi)	Ni–Bi	≈ 100 at. % Bi	$hR2$	$R\bar{3}m$	αAs	[28]
	Bi–Sn	≈ 100 at. % Bi				
NiBi	Ni–Bi	47–51 at. % Bi	$hP4$	$P6_3/mmc$	NiAs	[18, 20]
$NiBi_3$	Ni–Bi	≈ 75 at. % Bi	$oP16$	$Pnma$	$CaLiSi_2$	[18, 20]

*-metastable phases, obtained usually by electroplating of Ni–Sn alloys.

$$y^n = K\,t, \quad m^n \tag{1}$$

Here y is the width (m) of the layer(s) obtained in the contact zone between both parts of a diffusion couple, t-reaction time (s), and K-growth coefficient (m^n/s). Usually, the exponent n is equal to 2 or 1 (in case of parabolic and linear growth, respectively). The values of K and the exponent n can be calculated easily in logarithmic coordinates $\{\ln(y)$ vs. $\ln(t)\}$ for example.

The diffusion layer growth apparent activation energy (E_A) may be calculated by Arrhenius plot ($\ln(K)$ vs. $1/T$). Pertinent literature data have been summarised in Table 2 [2, 3, 5, 10, 35-43]. Significant variations are observed but an extensive discussion of the reasons would be out of the scope of this work. Nevertheless, we suggest the hypothesis that the apparent layers growth activation energy from liquid Sn-containing phase is different from the one assessed at growth from solid Sn-containing phase. More details are discussed in the Results and Discussion section of this work.

3. Experimental

Diffusion couples of solid/liquid type were prepared. Each solid part consisted of a prismatic Ni piece while the respective liquid part contained preliminary synthesized Bi–Sn alloy with a predetermined composition. Granules of Bi and Sn (p.a.) and 99.99 wt. % purity Ni each were used for the experiments.

The Ni prisms dimensions were approximately 8 x 8 x 10 mm. The latter were covered electrochemically by a thin Sn layer (around 3 μm thick) in order to facilitate the initial interface reaction and to diminish the influence of wettability variations due to the different chemical compositions of the Bi–Sn melts. The galvanic bath (200 cm^3) consisted of 1 N SnCl$_2$ with addition of HCl (in order to avoid precipitation of Sn hydroxides and to increase the electroconductivity). The measured acidity (pH) of the electrolytic solution had the value of pH = 1. Gelatin (2 g) was added to the bath in order to improve the electrodeposited layer quality [44]. Sn anode, Ni cathode and direct current density of 2 $A.dm$ were used.

Three various compositions (i.e. corresponding to different Bi/Sn ratios) of the Bi–Sn melts were chosen. Thus, samples nos. 1 to 6 contained 0.8; nos. 7 to 12-0.6; and nos. 13 to 18-0.4 mole fractions Sn. One should be aware that the chemical composition of the diffusion couple liquid parts of samples nos. 7-12 corresponds approximately to that one of the eutectic point (0.61 mole fractions Sn) in the Bi–Sn system [28, 45].

Evacuated borosilicate glass tubes, containing Bi and Sn (around 10 g) in the desired ratios and a piece

Table 2. *Literature data about the layers growth apparent activation energy, Ref – reference, E_A – value of the apparent growth activation energy, kJ mol⁻¹.*

No	Diffusion couple type	Growing phase	E_A/ kJ mol⁻¹	Temperature intervals (°C) and remarks	Ref
1	(Ni) / (βSn, Bi)	Ni$_3$Sn$_4$	90	85–120	[2]
2	(Ni) / (liquid Sn, Bi)	Ni$_3$Sn$_4$	23	180–360	[3]
3	(Ni) / (βSn, Bi)	Ni$_3$Sn$_4$	82	70–120	[5]
4	(Ni) / (liquid Sn, Bi)	Ni$_3$Sn$_4$	33	250–280	[10]
5	(Ni) / (liquid Sn)	Ni$_3$Sn$_4$	28	235–600	[35]
6	(Ni) / (βSn)	Ni$_3$Sn$_4$	116	160–200	[36]
7	(Ni) / (βSn)	Ni$_3$Sn$_4$	39	150–225; * ED NiSn phase observed after 55 d aging at room temperature	[37]
8	(Ni, 11.7 wt%P) / (βSn)	Ni$_3$Sn$_4$, Ni$_3$P	36	145–180	[38]
9	(Ni, P) / (βSn)	Ni$_3$Sn$_4$	42	120–200	[39]
10	(Ni) / (βSn-3.5Ag)	Ni$_3$Sn$_4$	16	150–200	[40]
11	* ED(Ni) / ED (βSn)	Ni$_3$Sn$_4$	58	100–150	[41]
		Ni$_3$Sn$_4$	91	150–175	
12	(Ni) / (βSn)	Ni$_3$Sn$_4$	30	75–160	[42]
	* ED(Ni) / ED (βSn)	Ni$_3$Sn$_4$	37	70–170	
13	(Ni) / (βSn)	Ni$_3$Sn$_4$	130	100–213	[43]
	(Ni) / ED (βSn)	Ni$_3$Sn$_4$	140	100–213	

* ED – electrodeposited.

of tin-coated nickel were prepared. The annealing of the diffusion couples was performed at 370 ± 1 °C for various times (24 to 216 h).

A resistance furnace (ERALY) supplied with 1/16 DIN type electronic regulator was used. At the working conditions the molten Bi–Sn alloy surrounds the solid Ni-prism, thus forming a liquid/solid $(Ni)_s/(Bi+Sn)_{liq}$ reaction couple. The latter subscripts denote "solid" and "liquid" phases, in the same order. After expiration of the desired reaction time the ampoules were taken out from the furnace and cooled in air. Preliminary experiments have shown that quenching the ampoules in cold water was not desirable because of the risk to break up in small pieces the liquid part of a specimen.

Afterward, every sample was mounted into epoxy resin, grounded and polished. The obtained cross-sections are normal to the contact solid/liquid surface of a diffusion couple. Further, the samples were examined by optical and by scanning electron microscope (SEM) using JEOL apparatus, type JSM 6390. The chemical composition of selected spots was measured by energy-dispersive spectroscopy (EDS) analysis (EDS Oxford INCA device, operated at 20 kV). The concentrations of Bi, Ni and Sn were obtained by quantifying the corresponding characteristic X-ray peaks (M_α, K_α and L_α, respectively). The concentrations of all components were measured simultaneously during 100 or 200 s. Only measurements with total atomic percentage within 100 ± 1 % were taken into account.

The overall thicknesses of the diffusion zones was determined by optical microscope (Olimpus) using a pertinent software package. For this purpose 20 to 40 separate values of the layers' width were taken into account for each sample. One should be aware that, at

this stage, we were not able to distinguish the different phase. The latter were identified by means of the above mentioned EDS analyses.

Vickers microhardness of selected phases was measured using a PMT-3 device, applying a diamond pyramid as indenter. This method allows choosing the spot (point) where the measurement is to be done. Therefore this technique is useful for phase characterization and identification (together with X-rays and EPMA analyses). In this study, a load of 20 g was applied during 15 s for each measurement. Every phase in a sample was measured from 3 to 8 times, depending on the scattering of the microhardness values. For the sake of verification the nickel phase microhardness of all samples has been measured. In consequence, an average value of 1.2 ± 0.2 GPa has been obtained, thus being in agreement with the data of Zhilyaev et al. [46] (1.4 GPa).

4.   Results and discussion

The contemporary conceptions about the relation between diffusion phenomena and the corresponding phase diagrams have been recently summarized by Ronka et al. [47], and by Kodentsov et al. [48]. Recently, Vassilev [49] has also implemented such an approach to the system Ti–Bi–Sn.

In most of the above mentioned studies only Ni_3Sn_4 layers formation was observed [1-5, 8-10]. Nevertheless, one has to be aware that the latter investigations have not been intended for phase diagram studies. According to us, attention has been paid mainly to the layers' growth kinetics and not so much to the precise determination of their phase compositions.
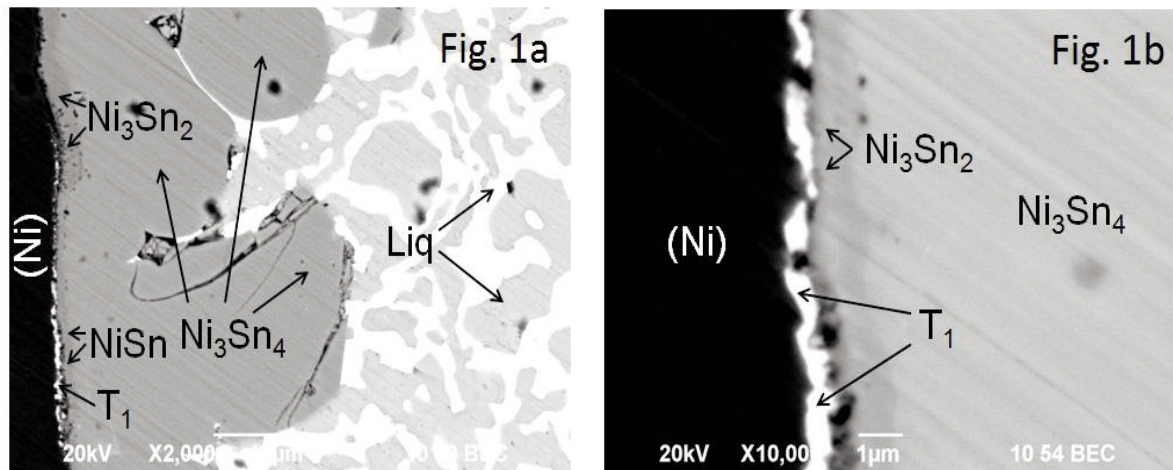
The experimental results obtained in this work are

Figure 1. *a, b. Micrographs of sample No. 11 (annealed at 370 °C) in back scattered electrons. a) The main diffusion layer is of Ni_3Sn_4 phase; the (former) liquid phase (Liq) consists of light (Bi-rich) and darker Sn-rich (areas); ternary phase (T_1) is observed as white layer between (Ni) and Ni_3Sn_2-layer; NiSn layer is situated between Ni_3Sn_2 and Ni_3Sn_4 layers. b) Magnified region of sample No. 11. The white layer belonging to the T_1 phase is well seen.*

exhibited in Tables 3a-c, respectively. In most cases the predominant phase is Ni_3Sn_4 except in sample No. 18. In numerous occasions compositions that was identified as a ternary compound (T_1) [24] were observed (sample nos. 4, 7, 10, 11, 17). The latter appears as a white ribbon (or white spots) next to the (Ni)-phase (Fig. 1a, b).

In Fig. 2 a micrograph showing the appearance of the metastable NiSn phase is represented.

As one can see (Tables 3 a-c) the diffusion paths go through the Ni–Sn side (i.e. Ni–Sn binary compounds are formed initially). Only at very long times and Bi-richest melts, binary Ni–Bi phases are formed in the diffusion zone (sample No. 18, Fig. 3).

Details of the chemical compositions determined by EDS analyses are presented in Tables 4 a–c. These data give the possibility (in combination with the

knowledge of the respective phase diagrams) to identify the phases grown in the contact zone. Average chemical compositions of each binary phase appearing in the diffusion layers and the respective standard deviations have been calculated.

The composition range of the ternary compound T_1 coincides roughly with that one given by Vassilev et al. [25]. Nevertheless, one should be aware that the homogeneity ranges of each phase, grown in the diffusion zone, are displaced relatively to these of the pertinent equilibrium phase diagrams. This might be a reason that the compositions associated with the T_1-phase, in this work (Tables 4 a-c) are pretty scattered. Another reason might be the existence of more than one ternary Ni–Bi–Sn compounds but the latter hypothesis could not be sustained presently. It is of worth noting also that the metastable phases NiSn and
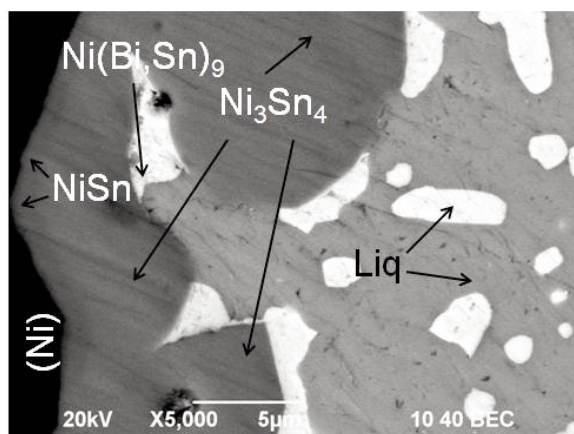

Figure 2. *Micrograph of sample No. 2, in back scattered electrons. The (former) liquid phase (Liq) consists of light (Bi-rich) and darker Sn-rich (areas).*
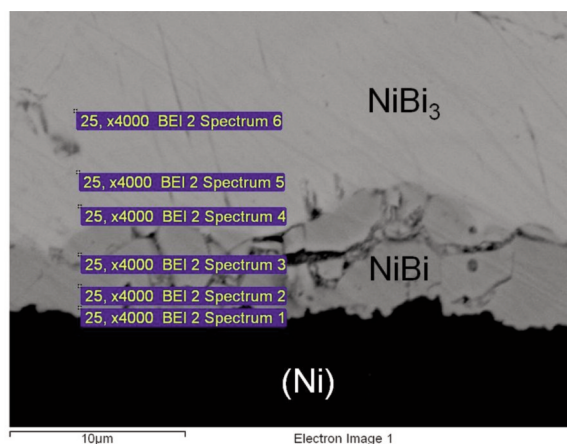

Figure 3. *Micrograph of sample No. 18 in back scattered electrons. Nickel-bismuth diffusion layers are exhibited only. The rectangles with notes "Spectrum xx" stand for the spots where point or area-analyses were done.*
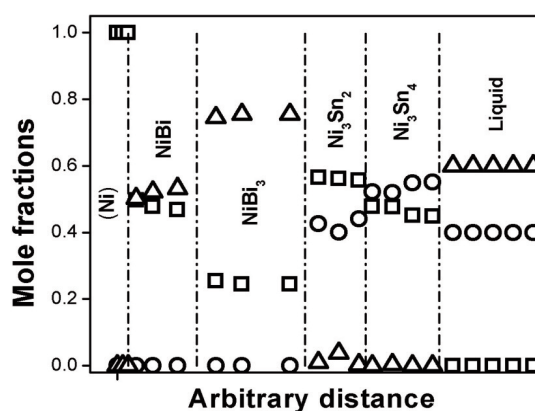
Figure 4. *Schematic representation of the diffusion zone composition profile of sample 18. Arbitrary distance is plotted along the abscissa, and the measured mole fractions of the constituents (X_{Bi}-△, X_{Ni}-□, X_{Sn}-○)-along the ordinate. The dash-dotted lines symbolize the interfaces between the layers*

Figure 5. *Micrograph of the liquid phase part of sample No. 15 in back scattered electrons. The darker areas are Sn-rich while the lighter are Bi-rich.*

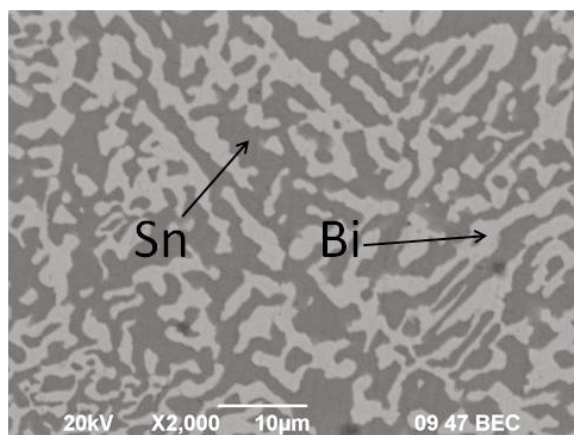***Table 3a.*** *Results obtained with diffusion couples having liquid parts Bi/Sn atomic ratio equal to 2 vs. 8. No - sample number; Time – duration of the annealing, s; Δy – diffusion zone thickness, m; Diffusion path – sequence of the phases in the diffusion zone (the largest layer is underlined); Remarks – supplementary notes. T1 – ternary phase, Liq – liquid phase*

No	Time / s	Δy / mx10^{-6}	Diffusion path	Remarks
1	86400	14.8 ± 3.4	(Ni) / Ni_3Sn_2 / NiSn*/ $\underline{Ni_3Sn_4}$ / Liq	* Layer corresponding to the metastable NiSn phase.
2	172800	20.1 ± 3.6	(Ni) / NiSn* / $\underline{Ni_3Sn_4}$ / Liq	* Layer corresponding to the metastable NiSn phase.Dendrite $Ni(Bi,Sn)_9$ observed in the liquid phase.
3	259200	22.4 ± 5.3	(Ni) / Ni_3Sn / NiSn* / $\underline{Ni_3Sn_4}$ / Liq	* Layer corresponding to the metastable NiSn phase.
4	432000	71.7 ± 17.0	(Ni) / T_1 / Ni_3Sn / Ni_3Sn_2 / NiSn* / $\underline{Ni_3Sn_4}$ / Liq	Ternary compound T_1 found. * Layer corresponding to the metastable NiSn phase.
5	604800	50.2 ± 7.0	(Ni) / Ni_3Sn / Ni_3Sn_2 / $\underline{Ni_3Sn_4}$ / Liq	Dendrite $Ni(Bi,Sn)_9$ observed in the liquid phase.
6	777600	74.7 ± 18.9	(Ni) / Ni_3Sn / $\underline{Ni_3Sn_4}$ / Liq	

Table 3b. *Results obtained with diffusion couples having liquid parts Bi/Sn atomic ratio equal to 4 vs. 6. No - sample number; Time – duration of the annealing, s; Δy – diffusion zone thickness, m; Diffusion path – sequence of the phases in the diffusion zone (the largest layer is underlined); Remarks – supplementary notes. T1 – ternary phase, Liq – liquid phase.*

No	Time / s	Δy / mx10^{-6}	Diffusion path	Remarks
7	86400	17.1 ± 5.2	(Ni) / T_1 / Ni_3Sn_2 / $\underline{Ni_3Sn_4}$ / Liq	Ternary compound T_1– found somewhere between (Ni) and diff. layer looking like white spots. Dendrite $Ni_{23}Bi_1Sn_{76}$ – found in the liquid phase
8	172800	20.3 ± 5.6	(Ni) / Ni_3Sn_2/ Ni_3Sn_4 / Liq	
9	259200	22.9 ± 5.7	(Ni) / Ni_3Sn_2/ NiSn* / $\underline{Ni_3Sn_4}$ / Liq	* Layer corresponding to the metastable NiSn phase.
10	432000	29.4 ± 7.3	(Ni) / T_1 /Ni_3Sn/ Ni_3Sn_2 / $\underline{Ni_3Sn_4}$/ Liq	T_1 found between (Ni) and Ni_3Sn looking like white spots. Dendrites $Ni_{17}Bi_{57}Sn_{26}$ and $Ni(Bi,Sn)_9$–found in liquid phase
11	604800	34.5 ± 7.0	(Ni) / T_1 / Ni_3Sn_2 / NiSn* / $\underline{Ni_3Sn_4}$/ Liq	T_1 found between (Ni) and Ni_3Sn looking like white spots. * Layers corresponding to the metastable NiSn phase.
12	777600	50.5 ± 11.6	(Ni) / $\underline{Ni_3Sn_4}$ / Liq	

Table 3c. *Results obtained with diffusion couples having liquid parts Bi/Sn atomic ratio equal to 6 vs. 4. No - sample number; Time – duration of the annealing, s; Δy – diffusion zone thickness, m; Diffusion path – sequence of the phases in the diffusion zone (the largest layer is underlined); Remarks – supplementary notes. Liq – liquid phase.*

No	Time / s	Δy / mx10^{-6}	Diffusion path	Remarks
13	86400	12.0 ± 2.2	(Ni) / Ni_3Sn/ Ni_3Sn_2 / NiSn* / $\underline{Ni_3Sn_4}$ / Liq	* Layer corresponding to the metastable NiSn phase. Dendrites with composition $Ni(Bi,Sn)_9$ in the liquid phase
14	172800	15.2 ± 3.0	(Ni) / $\underline{Ni_3Sn_4}$ / Liq	
15	259200	21.1 ± 5.4	(Ni) / Ni_3Sn / NiSn* / $\underline{Ni_3Sn_4}$ / Liq	* Layer corresponding to the metastable NiSn phase $Ni(Bi,Sn)_9$ and Ni-rich dendrites are observed in the liquid phase, near to the last diffusion layer
16	432000	46.0 ± 7.3	(Ni) / Ni_3Sn_2 / $\underline{Ni_3Sn_4}$ / Liq	
17	540000	53.0 ± 17.0	(Ni) / T_1/ Ni_3Sn_2 / NiSn* / $\underline{Ni_3Sn_4}$ / Liq	Ternary compound T_1– found somewhere between (Ni) and diff. layer looking like white spots. * Layer corresponding to the metastable NiSn phase. Dendrites $Ni(Bi,Sn)_9$ in the liquid phase
18	777600	524.8 ± 137.5	(Ni) / NiBi/ $\underline{NiBi_3}$ / Ni_3Sn_2/ Ni_3Sn_4 / Liq	Ni-rich dendrites are observed

$NiSn_9$ were observed at several occasions (Table 4 a-c).

As previously mentioned a "quaternary" IMC $Au_2Ni_{15}Sn_{77}Bi_6$ was reported by Cho et al. [9]. According to us this phase is related to the Ni–Sn–Bi system because it contains only 2 % of foreign (Au) atoms. It might be the metastable $NiSn_9$-phase.

The average chemical compositions of all Ni–Sn solid phases (Ni_3Sn, Ni_3Sn_2, NiSn, Ni_3Sn_4) identified by using SEM–EDS in the diffusion layers are, respectively: $X_{Ni} = 0.73 \pm 0.04$, $X_{Bi} = 0.01 \pm 0.01$, $X_{Sn} = 0.26 \pm 0.04$; $X_{Ni} = 0.58 \pm 0.01$, $X_{Bi} = 0.01 \pm 0.01$, $X_{Sn} = 0.41 \pm 0.01$; $X_{Ni} = 0.50 \pm 0.03$, $X_{Bi} = 0.00 \pm 0.01$, $X_{Sn} = 0.50 \pm 0.03$; $X_{Ni} = 0.42 \pm 0.02$, $X_{Bi} = 0.00 \pm 0.01$, $X_{Sn} = 0.58 \pm 0.02$. As expected these compositions deviate in some degree from the values given of the respective binary phase diagrams.

The measured Vickers microhardness values (HV, GPa) of Ni_3Sn_4 layers are exhibited in Table 4 a-c. They were compared with such data (unpublished) measured with samples used by the authors in a previous studies of the system Ni–Sn–Bi [27]. Some differences were observed between HV measured with equilibrated samples and those measured after DSC analyses of the same specimens. Such a divergence is attributed to the appearance of Ni3Sn2 phase in the latters.

Table 4a. *Results of analyses done by SEM–EDS with diffusion couples, containing liquid parts Bi/Sn atomic ratio equal to 2 vs. 8, annealed at 370 °C for various times. No.-specimen's number; X_i-constituents' mole fractions with the corresponding standard deviations SD_i; Phases-identified phases; Remarks and HV values-supplementary notes and measured microhardness values (HV, GPa) of the Ni_3Sn_4.*

No.	$X_{Ni} \pm SD_{Ni}$	$X_{Bi} \pm SD_{Bi}$	$X_{Sn} \pm SD_{Sn}$	Phases	Remarks and HV values
	0.880 ± 0.005	0.000 ± 0.005	0.120 ± 0.005	(Ni)	solid solution of Sn into (Ni)
	0.608 ± 0.005	0.000 ± 0.005	0.392 ± 0.005	Ni_3Sn_2_LT	
1	0.479 ± 0.015	0.000 ± 0.005	0.521 ± 0.015	NiSn	2 spectra
	0.416 ± 0.013	0.000 ± 0.005	0.584 ± 0.013	Ni_3Sn_4	3 spectra, HV = 3.93 ± 0.69 GPa
	0.006 ± 0.008	0.046 ± 0.032	0.948 ± 0.024	Liquid	dendrites, 2 spectra
	0.507 ± 0.039	0.000 ± 0.005	0.493 ± 0.039	NiSn	metastable phase
	0.420 ± 0.013	0.000 ± 0.005	0.580 ± 0.013	Ni_3Sn_4	7 spectra, HV = 4.53 ± 0.56 GPa
2	0.076 ± 0.005	0.064 ± 0.005	0.860 ± 0.005	$Ni(Bi,Sn)_9$	dendrites
	0.000 ± 0.005	0.448 ± 0.005	0.552 ± 0.005	Liquid	dendrites
	0.000 ± 0.000	0.035 ± 0.015	0.965 ± 0.015	Liquid	dendrites
	0.700 ± 0.005	0.000 ± 0.005	0.300 ± 0.005	Ni_3Sn_LT	
3	0.543 ± 0.005	0.000 ± 0.005	0.457 ± 0.005	NiSn	metastable phase
	0.395 ± 0.028	0.010 ± 0.008	0.595 ± 0.021	Ni_3Sn_4	7 spectra, HV = 3.57 ± 0.39 GPa
	0.000 ± 0.005	0.033 ± 0.005	0.967 ± 0.005	Liquid	dendrites
	0.651 ± 0.005	0.233 ± 0.005	0.116 ± 0.005	T_1	ternary compound
	0.582 ± 0.005	0.353 ± 0.005	0.065 ± 0.005	T_1	ternary compound
	0.691 ± 0.011	0.000 ± 0.005	0.309 ± 0.011	Ni_3Sn_LT	3 spectra
4	0.576 ± 0.030	0.003 ± 0.006	0.421 ± 0.029	Ni_3Sn_2_LT	5 spectra
	0.504 ± 0.005	0.000 ± 0.005	0.496 ± 0.005	NiSn	
	0.407 ± 0.017	0.000 ± 0.005	0.593 ± 0.017	Ni_3Sn_4	7 spectra, HV = 3.98 ± 0.34 GPa
	0.008 ± 0.007	0.082 ± 0.070	0.910 ± 0.070	Liquid	3 spectra
	0.745 ± 0.038	0.000 ± 0.005	0.255 ± 0.038	Ni_3Sn_LT	2 spectra
	0.590 ± 0.015	0.002 ± 0.004	0.408 ± 0.019	Ni_3Sn_2_LT	3 spectra
5	0.404 ± 0.008	0.000 ± 0.005	0.596 ± 0.008	Ni_3Sn_4	6 spectra, HV = 4.04 ± 0.48 GPa
	0.109 ± 0.005	0.019 ± 0.005	0.872 ± 0.005	$Ni(Bi,Sn)_9$	dendrites
	0.006 ± 0.009	0.054 ± 0.034	0.940 ± 0.025	Liquid	dendrites, 2 spectra
	0.920 ± 0.076	0.000 ± 0.005	0.080 ± 0.076	(Ni)	solid solution of Sn into (Ni), 3 spectra
	0.744 ± 0.005	0.000 ± 0.005	0.256 ± 0.005	Ni_3Sn_LT	
6	0.403 ± 0.005	0.000 ± 0.005	0.597 ± 0.005	Ni_3Sn_4	3 spectra, HV = 3.52 ± 0.59 GPa
	0.000 ± 0.005	0.941 ± 0.005	0.059 ± 0.005	Liquid	
	0.000 ± 0.005	0.025 ± 0.005	0.975 ± 0.005	Liquid	dendrites

Table 4b. _Results of analyses done by SEM–EDS with diffusion couples, containing liquid parts Bi/Sn atomic ratio equal to 4 vs. 6, annealed at 370 °C for various times. No. – specimen's number; Xi – constituents' mole fractions with the corresponding standard deviations SDi; Phases – identified phases; Remarks and HV values – supplementary notes and measured microhardness values (HV, GPa) of the Ni_3Sn_4._

No.	$X_{Ni} \pm SD_{Ni}$	$X_{Bi} \pm SD_{Bi}$	$X_{Sn} \pm SD_{Sn}$	Phases	Remarks and HV values
7	0.934 ± 0.005	0.039 ± 0.005	0.027 ± 0.005	(Ni)	solid solution of Sn into (Ni)
	0.887 ± 0.005	0.065 ± 0.005	0.048 ± 0.005	T_1	ternary compound
	0.852 ± 0.005	0.074 ± 0.005	0.074 ± 0.005	T_1	ternary compound
	0.831 ± 0.005	0.108 ± 0.005	0.061 ± 0.005	T_1	ternary compound
	0.685 ± 0.005	0.152 ± 0.005	0.163 ± 0.005	T_1	ternary compound
	0.589 ± 0.005	0.094 ± 0.005	0.317 ± 0.005	T_1	ternary compound
	0.552 ± 0.005	0.000 ± 0.005	0.448 ± 0.005	$Ni_3Sn_2\_LT$	
	0.410 ± 0.005	0.006 ± 0.008	0.584 ± 0.021	Ni_3Sn_4	2 spectra, HV = 2.58 ± 0.56 GPa
	0.230 ± 0.005	0.012 ± 0.005	0.758 ± 0.005	$Ni_{23}Bi_1Sn_{76}$	dendrites
8	0.579 ± 0.005	0.000 ± 0.005	0.421 ± 0.005	$Ni_3Sn_2\_LT$	2 spectra
	0.413 ± 0.007	0.000 ± 0.005	0.587 ± 0.007	Ni_3Sn_4	3 spectra, HV = 3.47 ± 0.59 GPa
	0.027 ± 0.023	0.953 ± 0.023	0.020 ± 0.018	Liquid	dendrites, 3 spectra
	0.023 ± 0.005	0.000 ± 0.005	0.977 ± 0.005	Liquid	dendrites
9	0.918 ± 0.005	0.007 ± 0.005	0.075 ± 0.005	(Ni)	solid solution of Sn into (Ni)
	0.631 ± 0.048	0.002 ± 0.005	0.367 ± 0.045	$Ni_3Sn_2\_LT$	2 spectra
	0.495 ± 0.005	0.013 ± 0.005	0.492 ± 0.005	NiSn	metastable phase
	0.413 ± 0.036	0.011 ± 0.015	0.576 ± 0.024	Ni_3Sn_4	3 spectra, HV = 4.26 ± 0.38 GPa
	0.000 ± 0.005	0.023 ± 0.005	0.977 ± 0.005	Liquid	dendrites
10	0.783 ± 0.005	0.196 ± 0.005	0.021 ± 0.005	T_1	ternary compound
	0.763 ± 0.005	0.237 ± 0.005	0.000 ± 0.005	T_1	ternary compound
	0.685 ± 0.005	0.300 ± 0.005	0.015 ± 0.005	T_1	ternary compound
	0.741 ± 0.042	0.020 ± 0.011	0.239 ± 0.030	Ni_3Sn_LT	2 spectra
	0.586 ± 0.008	0.008 ± 0.011	0.406 ± 0.019	$Ni_3Sn_2\_LT$	2 spectra
	0.426 ± 0.013	0.000 ± 0.005	0.574 ± 0.013	Ni_3Sn_4	2 spectra, HV = 3.44 ± 0.26 GPa
	0.168 ± 0.005	0.574 ± 0.005	0.258 ± 0.005	$Ni_{17}Bi_{57}Sn_{26}$	dendrites
	0.085 ± 0.005	0.148 ± 0.005	0.767 ± 0.005	$Ni(Bi,Sn)_9$	dendrites
	0.000 ± 0.005	0.027 ± 0.005	0.973 ± 0.005	Liquid	dendrites
11	0.669 ± 0.005	0.238 ± 0.005	0.093 ± 0.005	T_1	ternary compound
	0.627 ± 0.005	0.286 ± 0.005	0.087 ± 0.005	T_1	ternary compound
	0.603 ± 0.005	0.321 ± 0.005	0.076 ± 0.005	T_1	ternary compound
	0.565 ± 0.005	0.327 ± 0.005	0.108 ± 0.005	T_1	ternary compound
	0.574 ± 0.017	0.016 ± 0.019	0.410 ± 0.036	$Ni_3Sn_2\_LT$	5 spectra
	0.471 ± 0.005	0.000 ± 0.005	0.529 ± 0.005	NiSn	metastable phase
	0.402 ± 0.005	0.000 ± 0.005	0.598 ± 0.005	Ni_3Sn_4	HV = 4.29 ± 0.84 GPa
	0.016 ± 0.005	0.050 ± 0.005	0.934 ± 0.005	Liquid	dendrites
12	1.000 ± 0.005	0.000 ± 0.005	0.000 ± 0.005	(Ni)	solid solution of Sn into (Ni), 2 spectra
	0.415 ± 0.009	0.000 ± 0.005	0.585 ± 0.009	Ni_3Sn_4	8 spectra, HV = 3.06 ± 0.56 GPa
	0.000 ± 0.005	0.969 ± 0.005	0.031 ± 0.005	(Bi)	dendrites

Table 4c. *Results of analyses done by SEM–EDS with diffusion couples, containing liquid parts Bi/Sn atomic ratio equal to 6 vs. 4, annealed at 370 °C for various times. No. – specimen's number; Xi – constituents' mole fractions with the corresponding standard deviations SDi; Phases – identified phases; Remarks and HV values – supplementary notesand measured microhardness values (HV, GPa) of the Ni_3Sn_4.*

No.	$X_{Ni} \pm SD_{Ni}$	$X_{Bi} \pm SD_{Bi}$	$X_{Sn} \pm SD_{Sn}$	Phases	Remarks and HV values
13	0.773 ± 0.051	0.000 ± 0.005	0.227 ± 0.051	Ni_3Sn_LT	2 spectra
	0.580 ± 0.075	0.002 ± 0.005	0.418 ± 0.074	$Ni_3Sn_2\_LT$	2 spectra
	0.516 ± 0.005	0.000 ± 0.005	0.484 ± 0.005	NiSn	metastable phase
	0.422 ± 0.025	0.000 ± 0.005	0.578 ± 0.025	Ni_3Sn_4	4 spectra, HV = 3.61 ± 0.50 GPa
	0.111 ± 0.005	0.077 ± 0.005	0.812 ± 0.005	$Ni(Bi,Sn)_9$	dendrites
	0.096 ± 0.005	0.696 ± 0.005	0.208 ± 0.005	$Ni(Bi,Sn)_9$	dendrites
	0.063 ± 0.005	0.807 ± 0.005	0.130 ± 0.005	$Ni(Bi,Sn)_9$	dendrites
	0.049 ± 0.005	0.066 ± 0.005	0.885 ± 0.005	$Ni(Bi,Sn)_9$	dendrites
	0.039 ± 0.005	0.066 ± 0.005	0.895 ± 0.005	$Ni(Bi,Sn)_9$	dendrites
	0.000 ± 0.005	0.970 ± 0.042	0.030 ± 0.042	Liquid	dendrites
	0.000 ± 0.005	0.032 ± 0.005	0.968 ± 0.005	Liquid	dendrites
14	0.415 ± 0.007	0.000 ± 0.005	0.585 ± 0.007	Ni_3Sn_4	4 spectra, HV = 3.70 ± 0.26 GPa
	0.000 ± 0.005	0.981 ± 0.005	0.019 ± 0.005	Liquid	dendrites
	0.000 ± 0.005	0.041 ± 0.025	0.959 ± 0.025	Liquid	dendrites, 2 spectra
15	0.989 ± 0.005	0.000 ± 0.005	0.011 ± 0.005	(Ni)	solid solution of Sn into (Ni)
	0.715 ± 0.005	0.038 ± 0.005	0.247 ± 0.005	Ni_3Sn_LT	
	0.474 ± 0.024	0.000 ± 0.005	0.526 ± 0.024	NiSn	3 spectra
	0.410 ± 0.009	0.006 ± 0.012	0.584 ± 0.012	Ni_3Sn_4	4 spectra, HV = 3.68 ± 0.51 GPa
	0.316 ± 0.005	0.507 ± 0.005	0.177 ± 0.005	U	
	0.193 ± 0.005	0.449 ± 0.005	0.358 ± 0.005	U	Ni-rich dendrites
	0.283 ± 0.005	0.264 ± 0.005	0.453 ± 0.005	U	
	0.092 ± 0.005	0.610 ± 0.005	0.298 ± 0.005	$Ni(Bi,Sn)_9$	dendrites
	0.000 ± 0.005	0.323 ± 0.005	0.677 ± 0.005	Liquid	dendrites, integral spectrum
	0.030 ± 0.006	0.042 ± 0.009	0.928 ± 0.016	Liquid	dendrites, 2 spectra
16	0.559 ± 0.017	0.000 ± 0.005	0.441 ± 0.017	$Ni_3Sn_2\_LT$	3 spectra
	0.421 ± 0.005	0.000 ± 0.005	0.579 ± 0.005	Ni_3Sn_4	2 spectra, HV = 4.05 ± 0.40 GPa
	0.010 ± 0.005	0.023 ± 0.005	0.967 ± 0.005	Liquid	dendrites
17	0.696 ± 0.005	0.066 ± 0.005	0.238 ± 0.005	T_1	
	0.630 ± 0.005	0.190 ± 0.005	0.180 ± 0.005	T_1	
	0.534 ± 0.005	0.015 ± 0.005	0.451 ± 0.005	$Ni_3Sn_2\_LT$	
	0.534 ± 0.005	0.015 ± 0.005	0.451 ± 0.005	NiSn	
	0.384 ± 0.057	0.007 ± 0.009	0.609 ± 0.054	Ni_3Sn_4	4 spectra, HV = 4.36 ± 0.52 GPa
	0.128 ± 0.005	0.019 ± 0.005	0.853 ± 0.005	$Ni(Bi,Sn)_9$	dendrites
	0.000 ± 0.005	0.032 ± 0.005	0.968 ± 0.005	Liquid	dendrites
18	0.561 ± 0.005	0.017 ± 0.019	0.422 ± 0.020	$Ni_3Sn_2\_LT$	3 spectra
	0.459 ± 0.015	0.001 ± 0.005	0.540 ± 0.018	Ni_3Sn_4	4 spectra, HV = 4.03 ± 0.40 GPa
	0.481 ± 0.015	0.519 ± 0.015	0.000 ± 0.005	BiNi	3 spectra
	0.226 ± 0.043	0.774 ± 0.043	0.000 ± 0.005	Bi_3Ni	8 spectra
	0.492 ± 0.005	0.137 ± 0.005	0.371 ± 0.005	U	
	0.405 ± 0.005	0.307 ± 0.005	0.288 ± 0.005	U	
	0.339 ± 0.005	0.428 ± 0.005	0.233 ± 0.005	U	
	0.233 ± 0.005	0.611 ± 0.005	0.156 ± 0.005	U	Ni-rich dendrites
	0.216 ± 0.005	0.642 ± 0.005	0.142 ± 0.005	U	
	0.213 ± 0.005	0.638 ± 0.005	0.149 ± 0.005	U	
	0.000 ± 0.005	0.996 ± 0.007	0.004 ± 0.007	Liquid	dendrites, 7 spectra, one of the spectra is integral

U – unidentified phase.

Diffusion zone thickness as a function of time for all three compositions of the melts (80, 60 and 40 at. % Sn) have been measured in order to study the layers growth kinetics. Taking into account that the diffusion zones phase compositions are diverse it is easy to understand that the respective growth kinetics might not be similar. The exponent n (eq. 1) was calculated in logarithmic coordinates $\{\ln(y)$ vs. $\ln(t)\}$ (Fig. 6). The values of n thus obtained are: 1.3 ± 0.3, 2.2 ± 0.3 and 0.7 ± 0.2, respectively, for growth from melts containing 80, 60 and 40 at. % Sn. Thus, the parabolic growth rule is observed with sample nos. 7-12 only (i.e. growth from a melt containing 60 at. % Sn). The respective growth coefficient value calculated (assuming also a lack of incubation time) in

coordinates y vs. $t^{1/2}$ is (2.29 ± 0.02) x 10^{-15} m^2 s^{-1}.

It has been previously discussed that Ni_3Sn_4 layers growth kinetics had been intensively studied (Table 2). Nevertheless, in a few cases only the system Ni–Sn–Bi is concerned [2, 3, 5, 10]. Solid/liquid [3, 10] and solid/solid [2, 5] diffusion couples have been used. Literature growth coefficient values of the latter references together with that one assessed in this work have been plotted in Fig. 7 *vs.* the reciprocal temperature. The latter coefficient agrees well with the literature data of Tao [3] and Lin [10].

As one can see, the apparent growth activation energy assessed with literature data [2, 5] of Ni_3Sn_4 layers grown from solid state Sn–Bi mixtures is greater (88 ± 12 kJ mol^{-1}) than this one (18 ± 8 kJ mol^{-1}) calculated with layers grown from liquid Bi–Sn phase. Literature data of [3, 10] and results obtained in this work were used in the latter case. It should be mentioned too, that all aabove cited investigations [2, 3, 5, 10 and this work] have been performed with Bi–Sn (nearly-) eutectic composition samples.

This is a confirmation of the authors' hypothesis that the apparent layers growth activation energies depend on the physical conditions. Naturally, it has to be expected that the diffusion mobility in liquid state is greater than in solid state. That is why the supply of Bi and Sn atoms is facilitated in diffusion couple with liquid Bi–Sn phase and this circumstance influence the respective apparent activation energy value.

Figure 6. Dependence of the diffusion layers thickness (y, m) on the annealing time (t, s) in logarithmic coordinates. □ – Bi/Sn atomic ratio equal to 2 vs. 8, O – Bi/Sn atomic ratio equal to 4 vs. 6, △ – Bi/Sn atomic ratio equal to 6 vs. 4.
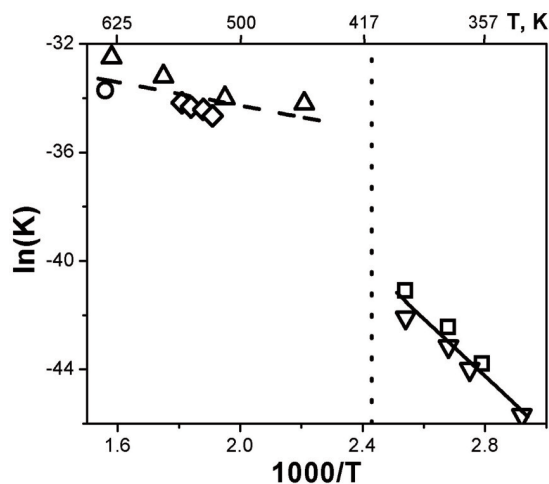

Figure 7. Arrhenius plot of the growth coefficients (K, m² s⁻¹). The dashed line represents the reciprocal Bi-Sn eutectic temperature value. The symbols stay for the respective results of △– Tao [3], ◇ – Lin [10], O – this work, □ – Chen [2] and ▽ – Yoon [5].

5. Conclusion

Diffusion couples consisting of solid nickel and liquid Bi–Sn phase have been constructed and studied at 370 °C. The phase and chemical compositions of the contact zone have been determined by means of scanning electron microscope. Diffusion paths have been identified and coupled with the ternary Ni–Sn–Bi phase diagram. It has been found that Ni_3Sn_4 is the main diffusion layer but other phase layers grow as well.

The appearance of a ternary compound previously reported in the literature has been confirmed. Metastable Ni–Sn phases (NiSn and $NiSn_8$ or $NiSn_9$) were observed in metallurgical samples (i.e. not by electroplating). Also it seems that a previously reported "quaternary" IMC ($Au_2Ni_{15}Sn_{77}Bi_6$) is related to the binary metastable phase $NiSn_{8(9)}$. Existence of more than one ternary Ni–Bi–Sn compounds might be admitted, probably, but such a hypothesis could not be sustained presently. The metastable phases NiSn and $NiSn_8$ ($NiSn_9$) have been observed too.

The apparent activation energy for growth from

liquid Bi–Sn phase is inferior to that one for growth from solid state Bi–Sn mixtures.

Acknowledgements

References

[1] S. Kang, R. Rai, S. Purushothaman, J. Electron. Mater. 25 (1996) 1113-1120.

[2] C. Chen, C. Ho, A. Lin, G. Luo, C. Kao, J. Electron. Mater. 29 (2000) 1200-1206.

[3] W. Tao, C. Chen, C. Ho, W. Chen, C. Kao, Chem. Mater. 13 (2001) 1051-1056.

[4] B.-L. Young, J.-G. Duh, J. Electron. Mater. 30 (2001) 878-884.

[5] J.-W. Yoon, C.-B. Lee, S.-B. Jung, Mater. Trans. 43 (2002) 1821-1826.

[6] M.Y. Chiu, S.Y. Chang, Y.H. Tseng, Y.C. Chan, T.H. Chuang, Z. Metallkd. 93 (2002) 248-252.

[7] J.-I Lee, S.-W. Chen, Hs.-Y. Chang, Ch.-M. Chen, J. Electron. Mater. 32 (2003) 117-122.

[8] J. Wang, H. Liu, L. Liu, Z. Jin, J. Electron. Mater. 35 (2006) 1842-1847.

[9] M. Cho, K. Paik, H. Lee, S. Booh, T.-G. Kim, J. Electron. Mater. 35 (2006) 35-40.

[10] Ch.-Y. Lin, Ch.-Ch Jao, Ch. Lee, Y.-W. Yen, JALCOM, 440 (2007) 333-340.

[11] H. Flandorfer, U. Saeed, C. Luef, A. Sabbar, H. Ipser, Thermochim. Acta, 459 (2007) 34-39.

[12] H. Ipser, H. Flandorfer, Ch. Luef, C. Schmetterer, U. Saeed, J. Mater. Sci.: Mater. Electron. 18 (2007) 3-17.

[13] W. Riesenkampf, T. Biestek, J. Morgiel, W. Lasocha, J. Mater. Sci. 36 (2001) 4633-4636.

[14] H.P. Rooksby, J. Electrodep. Tech. Soc. 27 (1951) 153-160.

[15] J.A. Augis, J.E. Bennett, J. Electrochem. Soc. 125 (1978) 335-339.

[16] C.C. Lo, J. Appl. Phys. 51 (1980) 2007-2013.

[17] M.H. Braga, J. Vizdal, A. Kroupa, J. Ferreira, D. Soares, L.F. Malheiros, CALPHAD 31 (2007) 468-478.

[18] G.P. Vassilev, X.J. Liu, K. Ishida, Journal of Phase Equilibria and Diffusion 26 (2005) 161-168.

[19] G.P. Vassilev, J. Romanowska, G. Wnuk, Intern. J. Mater. Res. 98 (2007) 468-475.

[20] G.P. Vassilev, K.I. Lilova, Cryst. Res. Technol. 42 (2007) 237-240.

[21] G.P. Vassilev, JALCOM 365 (2004) 164-167.

[22] G.P. Vassilev, K. Ishida, JALCOM 376 (2004) 125- 130.

[23] G.P. Vassilev, K.I. Lilova, J.-C. Gachon, J. Mining and Metallurgy (43) B (2007) 141-150.

[24] G.P. Vassilev, K.I Lilova, J.-C. Gachon, Cryst. Res. Technol. 43 (2008) 980-985.

[25] G.P. Vassilev, K.I. Lilova, J.-C. Gachon, JALCOM 469 (2009) 264-269.

[26] G. Vassilev, V. Gandova, N. Milcheva, G. Patronov, Annual of Shumen University, Chemistry XXI B1 (2011) 5-15.

[27] N. Milcheva, P. Broz, J. Buršík, G.P. Vassilev, Therm. Acta 534 (2012) 41-50.

[28] T. Massalski, Binary Alloy Phase Diagrams, ASM International, OH, USA, 1996 (CD ROM).

[29] T. Watanabe, Nano-Plating (2004).

[30] P. Nash, A. Nash, Bull. Alloy Phase Diagr. 6 (1985) 350-359.

[31] J.W. Cuthbertson, N. Parkinson, H.P. Rooksby, J. Electrochem. Soc. 100 (1953) 107-119.

[32] P.L. Cavallotti, L. Nobili, A. Vicenzo, Electrochim. Acta 50 (2005) 4557-4565.

[33] S. Bader, W. Gust, H. Hieber, Acta Metall. Mater. 43 (1995) 329-337.

[34] J. Shen, Y.C. Chan, S.Y. Liu, Acta Mater. 57 (2009) 5196-5206.

[35] D. Gur, M. Bamberger, Acta Mater. 46 (1998) 4917-4923.

[36] M. Mita, M. Kajihara, N. Kurokawa, K. Sakamoto, Mater. Sci. Eng. A 403 (2005) 269-275.

[37] W. Tang, A. He, Q. Kiu, D. Ivey, Intern. J. Minerals, Metallurgy and Materials 17 (2010) 459-463.

[38] J.Y. Song, J. Yu, T.Y. Lee, J. Mater. Res. 19 (2004) 1257-1264.

[39] S.J. Wang, H.J. Kao, C.Y. Liu, J. Electron. Mater. 33 (2004) 1130-1136.

[40] M.O. Alam, Y.C. Chan, J. Appl. Phys. 98 (2005) 123527-4.

[41] R. Labie, W. Ruythooren, J.V. Humbeeck, Intermetallics 15 (2007) 396-403.

[42] H. Blair, T. Pan, J. Nicholson, Electronic Components & Technology Conference, 48th IEEE, Seattle, WA, USA (1998) 259-267.

[43] D. Olsen, R. Wright, H. Berg, 13th Annual Proceedings on Reliability Physics, Las Vegas, NV, USA (1975) 80-86.

[44] M. Shcluger, Galvanic depositions in machine construction, Mashinostroenie, Moscow, 1985 (in Russian).

[45] A. Dinsdale, A. Watson, A. Kroupa, J. Vrestal, A. Zemanova, J. Vizdal, Atlas of Phase Diagrams for the Lead-Free Soldering, COST 531 (Lead-free Solders), Vol. 1, © COST office, 2008, ISBN 978-80-86292-28-1, Printed in the Czech Republic.

[46] A.P. Zhilyaev, S. Lee, G.V. Nurislamova, R.Z. Valiev, T.G. Langdon, Scripta Mater. 44 (2001) 2753-2758.

[47] K. Ronka, F.J.J. Van Loo, J.K. Kivilahti, Scripta Mat. 37 (1997) 1575-81.

[48] A. Kodentsov, G. Bastin, F.J.J. Van Loo, JALCOM 320 (2001) 207-217.

[49] G.P. Vassilev, Cryst. Res. Technol. 40 (2005) 713-718.